Self-Assembled Bis-Acridinium Tweezer Equilibria Controlled by Multi-Responsive Properties

Johnny Hu, Jean-pierre Launay, Alain Chaumont, Valérie Heitz, Henri-pierre Jacquot de Rouville

Chemistry–A European Journal
Research Article
doi.org/10.1002/chem.202401866
Chemistry Europe
European Chemical Societies Publishing
www.chemeurj.org

Self-Assembled Bis-Acridinium Tweezer Equilibria Controlled by Multi-Responsive Properties

Johnny Hu,[a] Jean-Pierre Launay,[b] Alain Chaumont,[c] Valérie Heitz,*[a] and Henri-Pierre Jacquot de Rouville*[a]

Protonated and methylated bis-acridinium tweezers built around a 2,6-diphenylpyridyl and an electron enriched 2,6-di(p-anisyl)pyridyl spacer have been synthesized. These tweezers can self-assemble in their corresponding homodimers and the associated thermodynamic parameters have been probed in organic solvents. The switching properties of the tweezers have been exploited in biphasic transfer experiments showing the shift of the equilibria towards the homodimers. Moreover, the thermodynamic parameters of the formation of the reduced methylated homodimers investigated by electrochemical experiments revealed the dissociation of the dimers. Thus, in addition to solvent and temperature, the pH and redox responsiveness of the acridinium units of the tweezers make it possible to modulate to a larger extent the monomer-dimer equilibria.

Introduction

Equilibria involving multiple interacting life components led to complex assemblies (double helix of DNA, G-quadruplex secondary structures, protein complexes).[1] These complex assemblies are endowed with numerous remarkable functions (transmission of information, chemical transformations, transport, regulation).[2,3] Recent years have seen the exploitation of the dynamic nature of supramolecular interactions to reach well-ordered assemblies based on self-organization of designed molecular entities.[4] In addition, various physical or chemical stimuli have been considered to modify equilibria of supramolecular systems to reach adaptive systems.[5] With no contests, stimuli-controlled equilibria represents the first step in the attractive fields of molecular machines[6] and constitutional dynamic systems.[7] In order to reach such complex systems, multi-switching properties are generally introduced and rely on the combination of several switching units[8] since few building blocks are intrinsically multi-responsive.[9] In this vein, the 9-arylacridinium unit is a motif of interest and is a multi-responsive unit in essence having redox, photochemical and halochromic properties.[10] In addition to its multi-switching properties, this relatively small heterocycle is a suitable recognition unit for π-donor molecules on account of its π-extended system and its electro-deficient nature.[11]

Scarcely incorporated in supramolecular architectures until now,[12] the 9-arylacridinium fragment was recently exploited as recognition units in molecular tweezers forming entwined dimers.[13] Even more surprisingly, tweezers of similar size and shape have led to a narcissistic self-sorting behavior.[14] In consequence, work still has to be done to understand the exact nature and strength of the weak interactions involved in these systems since self-assembling structures resulting from π-π interactions of identical tweezers usually lead to quadruple stacks, in solution and in the solid state.[15] In view of further use of this kind of molecular tweezer, it is thus important to study in detail their monomer-dimer equilibria in order to determine the best experimental conditions for their implementation as selective complexants.[16] To the best of our knowledge, switching properties were not used for rationalizing the interactions involved in these entwined assemblies. In addition, they are shown herein to be an asset for controlling self-assembly monomer-dimer equilibria and for understanding the contribution of dispersive and repulsive forces in the systems.

Here, we report the synthesis and the thermodynamic study of the monomer-dimer equilibria of four bis-acridinium tweezers $\mathbf{1}^{2+}$, $\mathbf{2}^{2+}$, $\mathbf{3}^{2+}$ and $\mathbf{4}^{2+}$ (Scheme 1). Besides the structure-property relationship of these tweezers, the switching properties of the acridinium core were probed by infrequent (or rarely attempted) experiments. We conducted i) biphasic experiments analyzed by ^{1}H NMR and molecular dynamics simulations and ii) variable temperature electrochemical experiments in order to elucidate the stabilizing interactions in the tweezers.

[a] J. Hu, V. Heitz, H.-P. Jacquot de Rouville
LSAMM, Institut de Chimie de Strasbourg, CNRS UMR 7177, Université de Strasbourg, 4, rue Blaise Pascal, 67000 Strasbourg, France
E-mail: v.heitz@unistra.fr
hpjacquot@unistra.fr

[b] J.-P. Launay
CEMES-CNRS, Université de Toulouse, 29 rue Jeanne Marvig, 31055 Toulouse, France

[c] A. Chaumont
Chimie de la Matière Complexe, CNRS UMR 7140, Université de Strasbourg, 4, rue Blaise Pascal, 67000 Strasbourg, France

Supporting information for this article is available on the WWW under https://doi.org/10.1002/chem.202401866

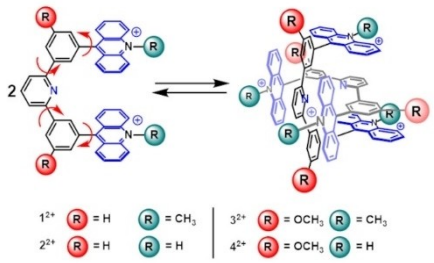

Scheme 1. Chemical structures of the molecular tweezers $\mathbf{1}^{2+}$, $\mathbf{2}^{2+}$, $\mathbf{3}^{2+}$ and $\mathbf{4}^{2+}$ in equilibrium with their entwined homodimers.

Results and Discussion

Monomer-Dimer Equilibrium Study

The ^{1}H NMR spectrum of **1·2CF$_3$COO** in CD$_3$OD (c = 5×10^{-4} mol L^{-1}, T = 293 K) showed the expected signals of the monomeric species (Figure 1). Upon increasing the concentration of **1·2CF$_3$COO** to 1×10^{-2} mol L^{-1}, the proton signals became broader and poorly resolved at the NMR time scale revealing a transition from a slow to an intermediate exchange regime (Figure S6.3). Based on the promising data reported in CD$_3$CN,[13] this behaviour was attributed to the equilibrium between the monomeric form of **1·2CF$_3$COO** and its corresponding dimer **(1)$_2$·4CF$_3$COO**. At 328 K, the spectrum characteristic of the monomer was observed at all concentrations (Figure S6.5). However, signals corresponding to a new species were recorded at 193 K (Figure S6.4). This new species was ascribed to the entwined dimer **(1)$_2$·4CF$_3$COO**. Formation of the entwined dimer **(1)$_2$·4CF$_3$COO** was corroborated by the upfield shift of the acridinium protons ($\Delta\delta(H_{1/8})$ = −0.94, $\Delta\delta(H_{2/7})$ = −0.48, $\Delta\delta(H_{3/6})$ = −0.15 and $\Delta\delta(H_{4/5})$ = −0.12 ppm) and the pyridinic protons ($\Delta\delta(H_\beta)$ = −1.07 and $\Delta\delta(H_\gamma)$ = −0.34 ppm) witnessing the involvement of π-stacking interactions. Thermodynamic parameters were assessed by variable temperature experiments of a diluted solution of **1·2CF$_3$COO** (c = 5×10^{-4} mol L^{-1}) in CD$_3$OD showing a mixture of monomer and dimer in slow exchange from 193 to 263 K. The determination of the binding constant (K_{Dim}) of dimerization at each temperature led to the estimation of the corresponding ΔG^0 parameter. Consequently, a van't Hoff plot analysis allowed the assessment of the enthalpic (ΔH^0 = −55.0 kJ mol^{-1}) and the entropic (ΔS^0 = −154.1 J mol^{-1} K^{-1}) contributions (Table 1, Figure S6.7). A similar behaviour was observed in CD$_3$CN[13,14] leading to ΔH^0 and ΔS^0 values of −48.3 kJ mol^{-1} and −130.7 J mol^{-1} K^{-1} respectively.

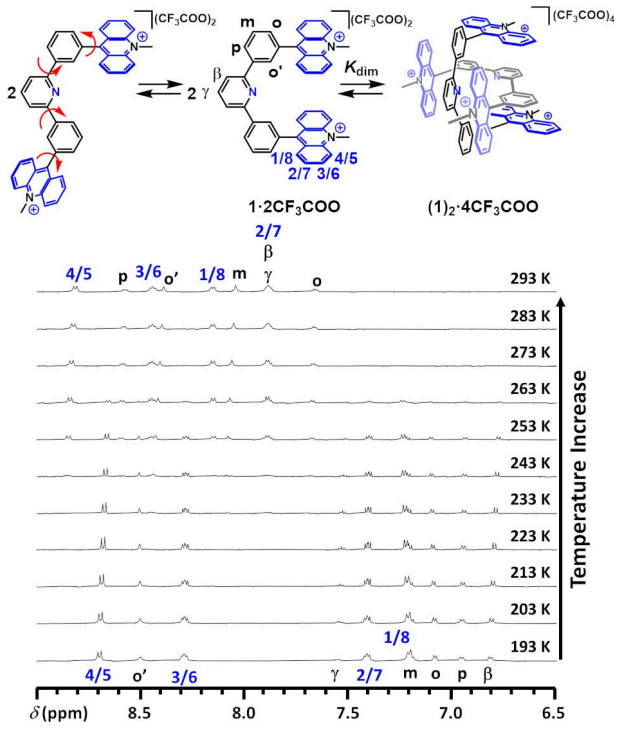

Figure 1. ^{1}H NMR spectra stack (600 MHz, CD$_3$OD) of **1·2CF$_3$COO** (c = 5×10^{-4} mol L^{-1}) at variable temperature (193 K to 293 K).

Structure-Properties Investigation

We were then interested in probing the influence of structural modifications in order to shed light on the interactions involved in the assembly. Following similar synthetic strategies as for $\mathbf{1}^{2+}$, a protonated $\mathbf{2}^{2+}$ tweezer and tweezers with electron enriched spacers $\mathbf{3}^{2+}$ and $\mathbf{4}^{2+}$ were synthesized (see ESI). First, the influence of the N–H proton in $\mathbf{2}^{2+}$ on the dimer formation in CD$_3$OD was investigated. Analogous chemical shifts were observed for the acridinium protons of **2·2Cl** ($\delta(H_{1/8})$ = 8.11, $\delta(H_{2/7})$ = 7.84 and $\delta(H_{3/6})$ = 8.33 ppm) compared to the previously reported N-methyl tweezers **1·2Cl** (Figures S4.5–S4.6).[14] A van't Hoff plot analysis on the protonated tweezer **2·2CF$_3$COO** was undertaken in CDCl$_3$, [D$_8$]THF, [D$_6$]acetone, CD$_3$CN, CD$_3$NO$_2$ and CD$_3$OD on account of its good solubility in different solvents (Figures S5.1–S5.18). It thus allows a direct comparison of the thermodynamic parameters in the different media using the empirical E_T(30) parameter (Table S5.7).[17,18] As a rule of thumb, the more the E_T(30) value of a solvent increases, the more stable the assembly (ΔG^0 decreases, K_{Dim} increases) with no **(2)$_2$·4CF$_3$COO** dimer formation observed in low polarity solvents, namely CDCl$_3$ and CD$_2$Cl$_2$. This empiric observation was confirmed except for CD$_3$OD. Since the same average geometry of the dimer is expected based on the low variation observed for the chemical shifts in various solvents (Figure S5.20), the less favoured enthalpic contribution ΔH^0 in CD$_3$OD is not the result of a change in the van der Waals interactions in the assembly but comes from solvation phenomena. When compared to **1·2CF$_3$COO**, this observation suggests that the labile N–H protons significantly i) impacts the solvent cohesive interactions as expected ($\Delta\Delta H^0$ = +25.8 kJ mol^{-1}) and ii) give rise to a stronger solvation of the monomer **2·2CF$_3$COO** ($\Delta\Delta S^0$ = +86.6 J mol^{-1} K^{-1}) in CD$_3$OD. Since **1·2CF$_3$COO** and **2·2CF$_3$COO** exhibits similar ΔH^0 and ΔS^0 in CD$_3$CN, it suggests that the protonated acridinium core does not alter π-π interactions in the assembly in comparison to the methylated acridinium unit.

Table 1. Least square line analysis of the van't Hoff plot of the monomer-dimer equilibrium of the 2,6-diphenylpyridyl tweezers **1·2CF$_3$COO**, **2·2CF$_3$COO** and 2,6-dianisylpyridyl tweezers **3·2CF$_3$COO** and **4·2CF$_3$COO** allowing the estimation of ΔH^0 (kJ mol^{-1}) and ΔS^0 (J mol^{-1} K^{-1}) in various solvents.

Compound	Solvent	ΔH^0 (kJ mol^{-1})	ΔS^0 (J mol^{-1} K^{-1})	ΔG^0 (kJ mol^{-1})	K_{Dim} at 298 K (L mol^{-1})	$E_T(30)$[a] (kJ mol^{-1})
1·2CF$_3$COO	CD_3OD	−55.0	−154.1	−9.1	39	231.9
2·2CF$_3$COO	CD_3OD	−29.2	−67.5	−9.1	39	231.9
2·2Cl	CD_3OD	−30.1	−72.6	−8.5	30	231.9
1·2CF$_3$COO	CD_3CN	−48.3	−130.7	−9.4	44	190.9
2·2CF$_3$COO	CD_3CN	−48.7	−127.4	−10.8	75	190.9
3·2CF$_3$COO	CD_3CN	−60.7	−162.0	−12.4	151	190.9
4·2CF$_3$COO	CD_3CN	−53.4	−117.9	−18.0[b]	1424[b]	190.9
2·2CF$_3$COO	[D$_6$]Acetone	−32.9	−77.9	−9.7	50	176.7
2·2CF$_3$COO	CD_3NO_2	−73.2	−225.4	−6.0	11	193.8
2·2CF$_3$COO	[D$_8$]THF	−20.6	−57.1	−3.6	4	156.6
2·2CF$_3$COO	CD_2Cl_2	–[c]	–[c]	–[c]	–[c]	170.4
2·2CF$_3$COO	$CDCl_3$	–[c]	–[c]	–[c]	–[c]	163.7

[a] $E_T(30)$ values taken from C. Reichardt, *Chem. Rev.*, **1994**, *94*, 2319–2358 (converted in kJ mol^{-1} for consistency reasons). [b] Experimental value determined by ^{1}H NMR spectroscopy. [c] Not determined since no dimers were formed at low temperatures.

Finally, tweezers **3·2CF$_3$COO** and **4·2CF$_3$COO** incorporating a 2,6-dianisylpyridyl spacer were studied to evaluate the effect of increasing electron density of the spacer on the enthalpic and entropic contributions to dimers formation (Figures S7.1–S8.7).[19] Both tweezers were studied in the most promising solvent for their dimer formation, namely CD_3CN.[20] They have more negative ΔG^0 values (K_{Dim} increase) than **1·2CF$_3$COO** and **2·2CF$_3$COO** reflecting an increased stabilization by van der Waals interactions (including π-π interactions). This observation validates the π-donor/π-acceptor hypothesis. However, addition of the methoxy groups on the spacer leads to an overall beneficial effect on both the enthalpic and entropic contribution of the equilibrium with an increased stabilisation of the dimer **(4)$_2$·4CF$_3$COO** over **(2)$_2$·4CF$_3$COO** by a factor of 18. The ability of the acridinium tweezers **2^{2+}** and **3^{2+}** to form their corresponding homodimers was also confirmed by X-ray diffraction (Figure 2).[21] These structures clearly show that protonated acridinium units and the 2,6-di(p-anisyl)pyridyl spacer can be involved in the formation of entwined dimers.

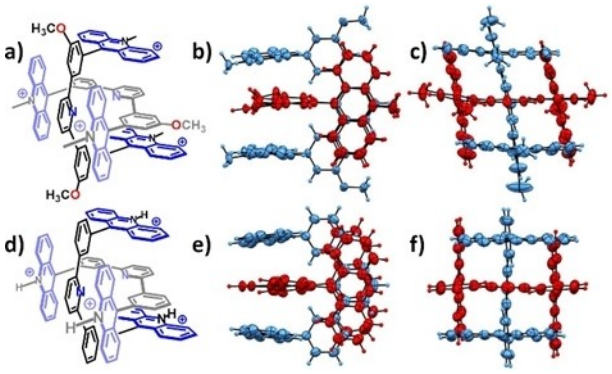

Figure 2. Crystal structure views (b and c) of **(3)$_2$·4PF$_6$** and (e and f) of **(2)$_2$·4Cl**. (a) Scheme of the entwined dimer of **(3)$_2$·4PF$_6$**. (b) Side view of the entwined dimer of **(3)$_2$·4PF$_6$** showing the π–π stacking between the acridinium moieties and the 2,6-dianisylpyridine spacer. (c) Rear view of the entwined dimer **(3)$_2$·PF$_6$**. (d) Scheme of the entwined dimer of **(2)$_2$·4Cl**. (e) Side view of the entwined dimer of **(2)$_2$·4Cl** showing the π–π stacking between the acridinium moieties and the 2,6-diphenylpyridine spacer. (f) Rear view of the entwined dimer **(2)$_2$·4Cl**.

Halochromic Properties and pH-Control of the Dimer Equilibria

The halochromic properties of the acridinium core were exploited to prepare the corresponding bis-acridane tweezer **5** (Figure 3). As expected, the bis-acridane tweezer **5** was isolated in a quantitative manner upon addition of a solution of KOH in CH_3OH to a solution of **1·2CF$_3$COO** in CH_3CN. The halochromic properties of the protonated acridinium cores were then probed in phase transfer experiments. These experiments were followed by slice selective ^{1}H NMR spectroscopy[22] and were performed on a biphasic mixture composed of a solution of bis-acridane tweezer **5** ($c = 5\times10^{-3}$ mol L^{-1}) in CD_2Cl_2 and D_2O (Figure 3).[23] Upon addition of D_2SO_4 ($c = 0.24$ mol L^{-1}), the successive disappearance of the signals of the tweezer **5** from the CD_2Cl_2 phase with the concomitant appearance of the **(2)$_2$·4DSO$_4$** dimer signals in the aqueous phase were observed. These observations clearly evidence the reversible halochromic properties of the tweezer on account of the rearomatization of its acridinium recognition units with no protonation of the central pyridine core as compared to the isolated spacers (Figure S3.80). However, no thermodynamic parameters can be estimated from this experiment since the formed deuterosulfate salt only remains partially soluble in the D_2O phase. Indeed, increasing the ionic strength of the aqueous phase leads to the precipitation of the **(1)$_2$·4DSO$_4$** dimer.[24] Nevertheless, a lower limit of the K_{Dim} value can be estimated at 10^5 L mol^{-1} from this

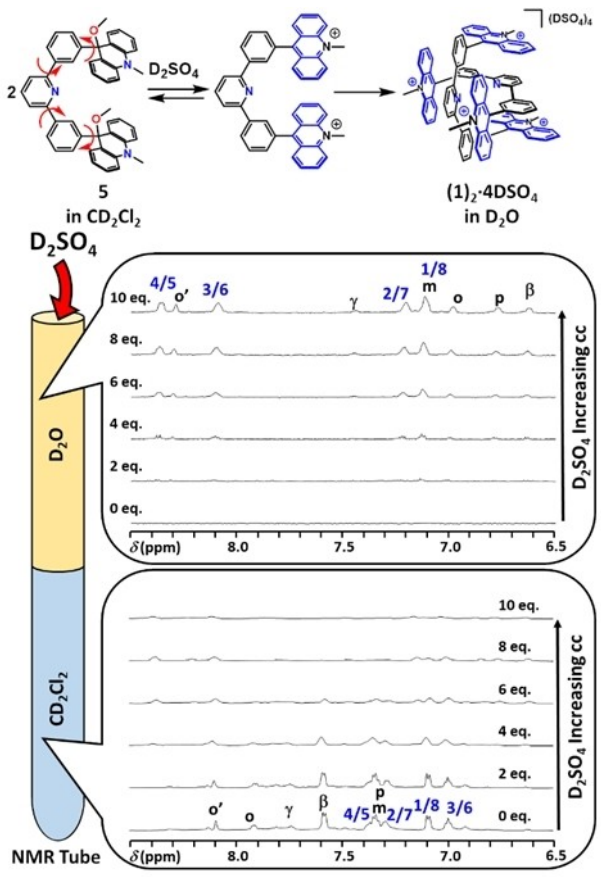

Figure 3. ^{1}H NMR (500 MHz, 298 K) slice selective stacks of a single biphasic NMR sample of a solution of tweezer **5** ($c = 5\times10^{-3}$ mol L^{-1}) in CD_2Cl_2 upon addition of a solution of D_2SO_4 ($c = 0.24$ mol L^{-1}) in D_2O in the D_2O phase.

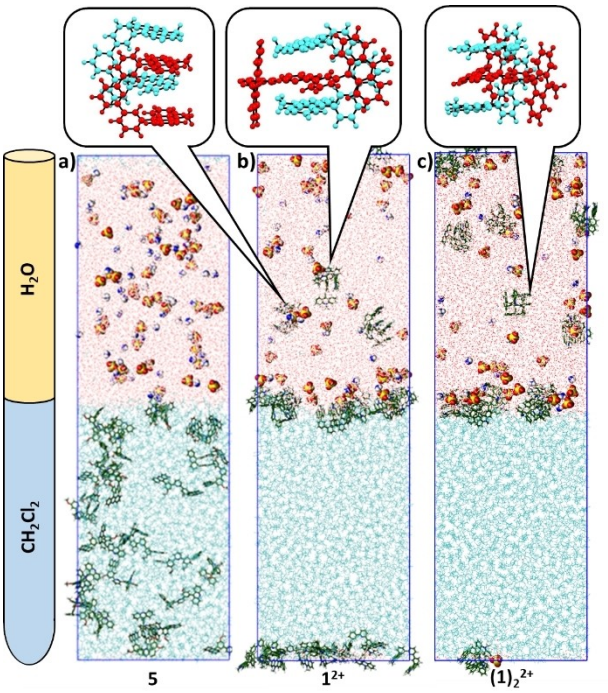

Figure 4. Classical molecular dynamics simulations of interfacial H_2O/CH_2Cl_2 systems of a) **5**, b) $\mathbf{1}^{2+}$ and c) $(\mathbf{1}^{2+})_2$ (box size 59.3 Å×59.3 Å×197.5 Å).

experiment considering that 10% of the unprobed protons in the D_2O phase corresponds to the monomeric species. The formation of the homodimers in D_2O under these conditions (concentration and temperature) clearly demonstrates the additional stabilization coming from the solvophobic effect of D_2O. An analogous behaviour was monitored for the other tweezers with similar estimated K_{Dim} values (see SI, Figures S10.1–S10.4). This observation is noticeable on account of the different chemical transformations involving either an elimination followed by rearomatization (N-methyl tweezers) or a protonation (N–H tweezers).

Classical molecular dynamics (cMD) simulations were performed in order to give further insights on the mechanism involved in these biphasic experiments (Figures 4 and S10.7–S10.10). Three case studies were considered for H_2O/CH_2Cl_2 interfacial systems containing the unprotonated tweezer **5**, the protonated tweezer $\mathbf{1}^{2+}$ and the dimer $(\mathbf{1}^{2+})_2$ in CH_2Cl_2 in the presence of $\mathbf{SO_4}^{2-}$ and $\mathbf{H_3O}^{+}$ ions in H_2O. The first case study revealed that neutral bis-acridane tweezers **5** reside in bulk CH_2Cl_2 and temporarily go at the interface (Figure 4a). As expected, H_3O^+ cations are exclusively in the H_2O phase thus suggesting that the protonation of **5** takes place at the interface. The second case study showed that after protonation, $\mathbf{1}^{2+}$ mainly resides at the interface behaving as surfactants (Figure 4b).[25] As a result of the saturation of the interface, they also migrate in the aqueous phase in the form of several transient dimers different from $(\mathbf{1}^{2+})_2$. In other words, the final dimer $(\mathbf{1}^{2+})_2$ is thus formed from equilibria evolving on a larger timescale than that of the cMD simulations. Finally, when preformed dimers $(\mathbf{1}^{2+})_2$ were introduced in the system, they partitioned between the interface and the aqueous phase (Figure 4c). The percentage of dimers extracted in the aqueous phase was estimated to be 16% in the case of $(\mathbf{1}^{2+})_2$.[26] However, the remaining presence of some of dimers at the interface may also explain the low solubility observed experimentally. It should be noted that we have reported an analogous behaviour for a tetracationic macrocyclic hosts.[27] It is worthwhile to note that simulations led to a similar behaviour for all four different tweezers (Table S10.1 and Figures S10.7–S10.10). Overall, these phase transfer experiments and simulations show how the halochromic properties of acridinium based systems can be exploited to shift the equilibrium to single homodimer species.

Redox Control of the Dimer Equilibria

The dimer-monomer equilibria of the different tweezers were investigated by cyclic voltammetry experiments under monomeric conditions according to NMR experiments (CH_3CN, $c = 0.5\times10^{-3}$ mol L^{-1}, $T = 308$ K). For instance, tweezers $\mathbf{1{\cdot}2PF_6}$ exhibits a reversible reduction wave ($E_{1/2} = -0.919$ V *vs.* Fc^+/Fc, $\Delta E = 75$ mV, Figure 5). UV/Vis spectroelectrochemical experiments reveal the full and reversible conversion of $\mathbf{1{\cdot}2PF_6}$ in $\mathbf{1}^{2\bullet}$ with the increase of the signature bands at 488 ($\varepsilon = 9$

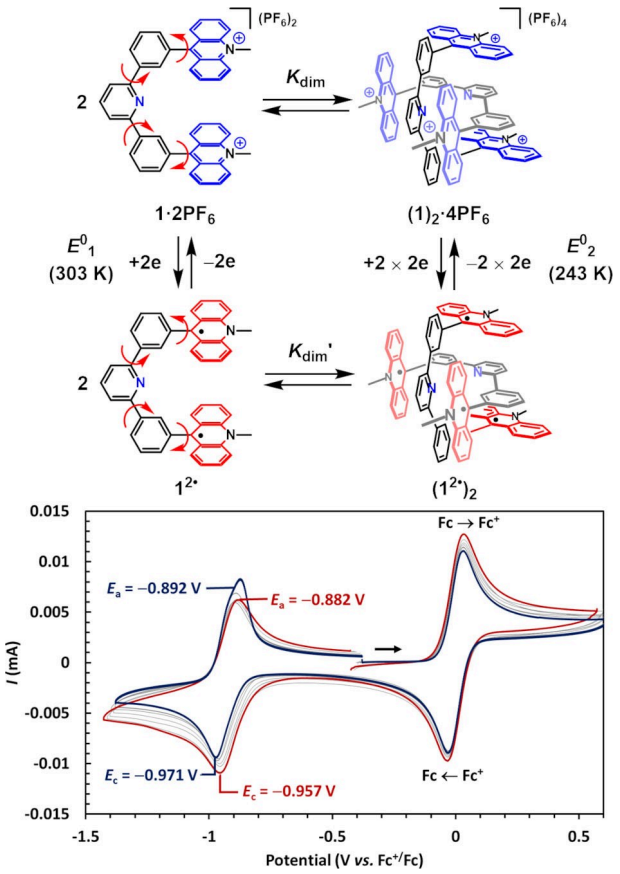

Figure 5. Cyclic voltammograms (CH_3CN, WE: Pt, CE: Pt, RE: Ag, 100 mV s^{-1}) of a solution of **1·2PF$_6$** ($c = 5\times10^{-4}$ mol L^{-1}) at 303 K (red), 293 K, 283 K, 273 K, 263 K, 253 K and 243 K (blue) in the presence of $TBAPF_6$ as supporting electrolyte ($c = 0.1$ mol L^{-1}). Potentials were referenced against Fc^+/Fc.

Table 2. Measured redox potentials $E_{1/2}$ (V *vs* Fc^+/Fc) of **1·2PF$_6$**, **3·2PF$_6$**, **PhAcr·PF$_6$** and **CH_3OPhAcr·PF$_6$**, the peak-to-peak difference (ΔE) and the binding constants of the monomer-dimer equilibrium of the methylated tweezer **1·2PF$_6$** and **3·2PF$_6$** estimated by ΔH^0 (kJ mol^{-1}) and ΔS^0 (J mol^{-1} K^{-1}) values of each system (thus giving ΔG^0 and K_{Dim} at 243 K), combined with the corrected shift $\Delta\Delta E_{1/2}$ of the reduction potential to obtain K'_{Dim}.

Compound	**1·2PF$_6$**	**3·2PF$_6$**	**PhAcr·PF$_6$**	**CH_3OPhAcr·PF$_6$**
$E_{1/2}$ (V), 303 K	−0.919	−0.928	−0.930	−0.933
ΔE (mV), 303 K	75	66	57	58
$E_{1/2}$ (V), 243 K	−0.931	−0.970	−0.927	−0.939
ΔE (mV), 243 K	79	101	62	58
$\Delta E_{1/2}$ (mV)	−12	−42	−6	+3
$\Delta\Delta E_{1/2}$ (mV)	−6	−45	–	–
K_{Dim} (L mol^{-1})	3591	38543	–	–
K_{Dim}' (L mol^{-1})	1141	7	–	–

300 L mol^{-1} cm^{-1}) and 525 (9 600) nm and the decrease of the bands at 405 (11 300), 427 (12 400) and 448 (8 800) nm (Figures S11.4–S11.6).[28] Variable temperature experiments were performed to probe the potential of the **(1)$_2$·4PF$_6$** dimer (Figure 5 and S11.3). Upon lowering the temperature to 243 K, a cathodic shift of the reduction potential was observed ($E_{1/2} = -0.931$ V *vs.* Fc^+/Fc, $\Delta E = 79$ mV). This observation can be rationalized by the formation of the **(1)$_2$·4PF$_6$** dimer. The cathodic shift from 303 to 243 K ($\Delta E_{1/2} = -12$ mV) evidences that the spacer transfers some of its electronic density to the acridinium cores making them harder to reduce thus reflecting the stabilization by the dimer formation.

A similar behaviour was observed for the electron enriched tweezer **(3)$_2$·4PF$_6$** and the corresponding model compound **CH_3OPhAcr·PF$_6$** (Figures S11.7–11.31). As expected, a more pronounced cathodic shift ($\Delta E_{1/2} = -42$ mV) was observed for **(3)$_2$·4PF$_6$** at 243 K than at 303 K on account of the higher dimer stability compared with **(1)$_2$·4PF$_6$**. This behavior can be best depicted according to a square scheme analysis (Figure 5). As a consequence, the association constant between reduced tweezers (K'_{Dim}) can be determined at 243 K from K_{Dim}, E°_1 (monomer redox potential) and E°_2 (dimer redox potential, Tables 2 and S11.1). The former can be estimated from the cyclic voltammetry curve ($E_{1/2}$) at 303 K, for which the monomer predominates, while the latter is measured at 243 K where the dimer predominates. However, there can be other sources of potential variations with temperature, such as changes in Fc^+/Fc potential, or entropy changes in the reduction reactions. To compensate for these effects, the raw $\Delta E_{1/2}$ change with temperature of **1·2PF$_6$** and **3·2PF$_6$** was subtracted by the $\Delta E_{1/2}$ change observed for the model compounds (unable to dimerize) **PhAcr·PF$_6$** and **CH_3OPhAcr·PF$_6$** (Table 2, line 5). The corrected value $\Delta\Delta E_{1/2}$ leads to an estimated K'_{Dim} value of two orders of magnitude lower for **(3$^{2\bullet}$)$_2$** ($K'_{Dim} \approx 7$ L mol^{-1}) than for **(1$^{2\bullet}$)$_2$** ($K'_{Dim} \approx 1141$ L mol^{-1}). In other words, the interaction between the electron enriched 2,6-dianisylpyridyl spacer and the reduced acridinium cores is disfavored in **(3$^{2\bullet}$)$_2$** in comparison to the 2,6-diphenylpydidyl spacer in **(1$^{2\bullet}$)$_2$**. This observation reveals that π-π coulombic repulsion predominates upon reduction leading to the dissociation of the assembly.

The large changes in dimerization constants K_{Dim} and K_{Dim}' can be further understood by means of a double mutant cycle (Figure 6).[29] The change in the free enthalpy of dimerization allows the rationalization of the interactions involved in the entwined assemblies upon substitution of the semi-rigid spacer unit ($\Delta\Delta G_{I\text{-}II}$ and $\Delta\Delta G_{III\text{-}IV}$) or by reduction of the acridinium cores ($\Delta\Delta G_{I\text{-}III}$ and $\Delta\Delta G_{II\text{-}IV}$). The $\Delta\Delta G$ terms for the substitution steps (horizontal arrows) give an idea on the electronic stabilizing contribution brought by both OCH_3 in the oxidized state ($\Delta\Delta G_{I\text{-}II} = -4.79$ kJ mol^{-1}) and on their repulsive contribution in the reduced state ($\Delta\Delta G_{III\text{-}IV} = +10.26$ kJ mol^{-1}). In addition, the opposite signs in these $\Delta\Delta G$ terms support that reduced acridinium sites exhibit a donor character and that interaction with the spacer becomes repulsive. More interestingly, the $\Delta\Delta G$ terms for the reduction steps (vertical arrows) are both positive but with a very different magnitude ($\Delta\Delta G_{I\text{-}III} = +2.32$ and $\Delta\Delta G_{II\text{-}IV} = +17.37$ kJ mol^{-1}). These differences show that both types of perturbations–substitution on the spacer and reduction of the acridinium groups–are acting additively. These observations are consistent with the major role played by π-donor/π-acceptor interactions in the dimerization process. These interactions can be tuned though the combination of two different modifications, i.e. modification of a donor group on one part of the

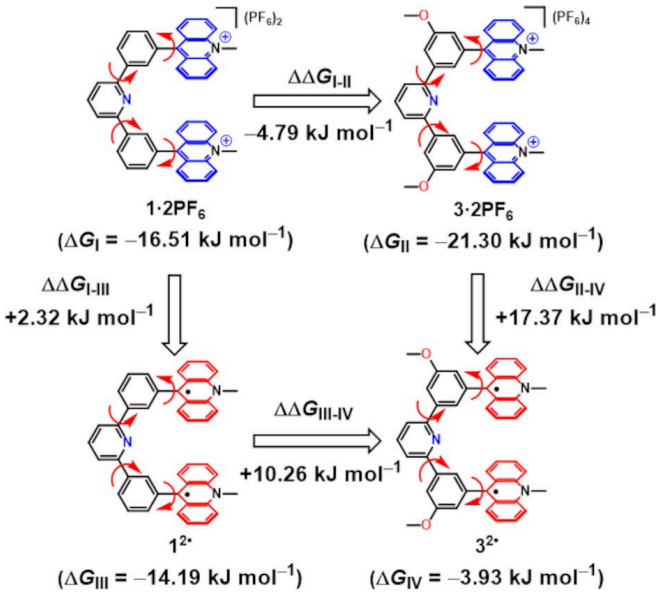

Figure 6. Double mutant cycle showing the changes in free enthalpy of dimerization for the molecules **1·2PF$_6$**, **3·2PF$_6$**, **1$^{2\bullet}$** and **3$^{2\bullet}$** in CH_3CN built from K_{Dim} and K_{Dim}' of Table 2 (with $\Delta\Delta G_{i\text{-}j} = -RT\ \ln(K_j/K_i)$ at 243 K).

molecule or a modification of an acceptor group in another part.

Conclusions

The synthesis, characterization and the self-assembly processes of bis-acridinium tweezers incorporating 2,6-diphenylpydidyl and 2,6-dianisylpyridyl spacers were performed. The associated thermodynamic studies demonstrated that π-donor/π-acceptor interactions between the spacer and the acridinium recognition units can be controlled i) classically by temperature and solvent and ii) by chemical and redox stimuli. In addition, protonated acridinium cores proved to be efficient for stabilizing the self-assembly and were successfully used as pH-switching units in phase transfer experiments. In addition to the chemical stimulus, injection of electrons in the methylated tweezers proved to be efficient for switching the monomer-dimer equilibrium. Finally, electrochemical experiments on the methylated tweezers also provided additional proofs on the involvement of π-donor/π-acceptor interactions in these entwined dimers. Altogether, these systems display a fine control of their dimer formation triggered by chemical (protons, solvent) and physical (redox, temperature) or a combination of these stimuli. The richness of the present series of compounds is essentially due to the possible modulation of the acridinium core by pH or redox switching. Supporting Information Summary

The authors have cited additional references within the Supporting Information.[30-42]

Author Contributions

Validation: JH; Supervision, Visualization, Writing–original draft, Data Curation, Investigation, Methodology, Project Administration: HPJR; Writing–Review and Editing, Conceptualization: JPL, AC, VH, HPJR; Data Analysis: JPL, HPJR; Resources: VH, HPJR; Funding acquisition: JH, VH, HPJR.

Acknowledgements

This work was supported by the CNRS and the University of Strasbourg. We gratefully acknowledge the Interdisciplinary Thematic Institute SysChem via the IdEx Unistra (ANR-10-IDEX-0002) within the program Investissement d'Avenir and the ANR (APGG 2022, ACROSS, ANR-22-CE07-0014) for financial support. We are grateful to the Fédération de Chimie Le Bel FR 2010 of the University of Strasbourg. JH thanks the French Ministry of National Education for a PhD Fellowship.

Conflict of Interests

The authors declare no conflict of interest.

Data Availability Statement

The data that support the findings of this study are available in the supplementary material of this article.

Keywords: Molecular tweezers · Entwined dimer · Acridinium · Halochromism · Electrochemistry

[1] a) N. A. Campbell, J. B. Reece, M. R. Taylor, E. J. Simon, J. L. Dickey, *Biology: Concepts and Connections*, Benjamin/Cummings Publishing Company, San Francisco, CA, 6th edn, **2008**; b) P. Sartori, S. Leibler, *Proc. Natl. Acad. Sci. U. S. A.* **2020**, *117*, 114–120.
[2] J. J. R. Fráusto da Silva, R. J. P. Williams, *The Biological Chemistry of the Elements, the Inorganic Chemistry of Life*, Chapter 10 Oxford University Press, Oxford, **1991**.
[3] N. O. Concha, J. F. Head, M. A. Kaetzel, J. R. Dedman, B. A. Seaton, *Science* **1993**, *261*, 1321–1324.
[4] a) P. T. Corbett, J. Leclaire, L. Vial, K. R. West, J.-L. Wietor, J. K. M. Sanders, S. Otto, *Chem. Rev.* **2006**, *106*, 3652–3711; b) J.-M. Lehn, *Angew. Chem. Int. Ed.* **2013**, *52*, 2836–2850.
[5] a) J. Berná, D. A. Leigh, M. Lubomska, S. M. Mendoza, E. M. Pérez, P. Rudolf, G. Teobaldi, F. Zerbetto, *Nat. Mater.* **2005**, *4*, 704–710; b) R. Eelkema, M. M. Pollard, J. Vicario, N. Katsonis, B. Serrano Ramon, C. W. M. Bastiaansen, D. J. Broer, B. L. Feringa, *Nature* **2006**, *440*, 163; c) T. Kudernac, N. Ruangsupapichat, M. Parschau, B. Maciá, N. Katsonis, S. R. Harutyunyan, K.-H. Ernst, B. L. Feringa, *Nature* **2011**, *479*, 208–211; d) L. Feng, Y. Qiu, Q.-H. Guo, Z. Chen, J. S. W. Seale, K. He, H. Wu, Y. Feng, O. K. Farha, R. D. Astumian, J. F. Stoddart, *Science* **2021**, *374*, 1215–1221
[6] a) J.-P. Sauvage, *Angew. Chem. Int. Ed.* **2017**, *56*, 11080–11093; b) J. F. Stoddart, *Angew. Chem. Int. Ed.* **2017**, *56*, 11094–11125; c) B. L. Feringa, *Angew. Chem. Int. Ed.* **2017**, *56*, 11060–11078.
[7] a) J.-M. Lehn, *Chem. Soc. Rev.* **2007**, *36*, 151–160; b) M. Barboiu, J.-M. Lehn, *Isr. J. Chem.* **2013**, *53*, 9–10.
[8] a) D. P. Funeriu, J.-M. Lehn, K. M. Fromm, D. Fenske, *Chem. – Eur. J.* **2000**, *6*, 2103–2111; b) A. Goodman, E. Breinlinger, M. Ober, V. M. Rotello, *J. Am. Chem. Soc.* **2001**, *123*, 6213–6214; c) G. Szalóki, G. Sevez,

J. Berthet, J.-L. Pozzo, S. Delbaere, *J. Am. Chem. Soc.* **2014**, *136*, 13510–13513; d) S. Gaikwad, A. Goswami, S. De, M. Schmittel, *Angew. Chem. Int. Ed.* **2016**, *55*, 10512–10517; e) B. Doistau, L. Benda, J.-L. Cantin, L.-M. Chamoreau, E. Ruiz, V. Marvaud, B. Hasenknopf, G. Vives, *J. Am. Chem. Soc.* **2017**, *139*, 9213–9220; f) R. Rabelo, S.-E. Stiriba, D. Cangussu, C. L. M. Pereira, N. Moliner, R. Ruiz-García, J. Cano, J. Faus, Y. Journaux, M. Julve, *Magnetochemistry* **2020**, *6*, 69.

[9] a) R. Klajn, *Chem. Soc. Rev.* **2014**, *43*, 148–184; b) J. D. Steen, D. R. Duijnstee, A. S. Sardjan, J. Martinelli, L. Kortekaas, D. Jacquemin, W. R. J. Browne, *Phys. Chem. A* **2021**, *125*, 3355–3361; c) S. L. Gilat, S. H. Kawai, J.-M. Lehn, *Chem. – Eur. J.* **1995**, *1*, 275–284; d) S. Cobo, F. Lafolet, E. Saint-Aman, C. Philouze, C. Bucher, S. Silvi, A. Credi, G. Royal, *Chem. Commun.* **2015**, *51*, 13886–13889; e) G. Moncelsi, P. Ballester, *ChemPhotoChem* **2019**, *3*, 304–317; f) F. Pina, M. J. Melo, C. A. T. Laia, A. J. Parola, J. C. Lima, *Chem. Soc. Rev.* **2012**, *41*, 869–908.

[10] H.-P. Jacquot de Rouville, J. Hu, V. Heitz, *ChemPlusChem* **2021**, *86*, 110–129.

[11] a) S. Claude, J.-M. Lehn, F. Schmidt, J.-P. Vigneron, *J. Chem. Soc. Chem. Commun.* **1991**, 1182–1185; b) A. Petitjean, R. G. Khoury, N. Kyritsakas, J.-M. Lehn, *J. Am. Chem. Soc.* **2004**, *126*, 6637–6647; c) M. Tanaka, K. Ohkubo, C. P. Gros, R. Guilard, S. Fukuzumi, *J. Am. Chem. Soc.* **2006**, *128*, 14625–14633; d) A. Chaudhary, S. P. Rath, *Chem. Eur. J.* **2012**, *18*, 7404–7417.

[12] a) W. Abraham, K. Buck, M. Orda-Zgadzaj, S. Schmidt-Schäffer, U.-W. Grummt, *Chem. Commun.* **2007**, 3094–3096; b) A. Vetter, W. Abraham, *Org. Biomol. Chem.* **2010**, *8*, 4666–4681; c) Y. Duo, S. Jacob, W. Abraham, *Org. Biomol. Chem.* **2011**, *9*, 3549–3559; d) K. Kurihara, K. Yazaki, M. Akita, M. Yoshizawa, *Angew. Chem. Int. Ed.* **2017**, *56*, 11360–11364.

[13] H.-P. Jacquot de Rouville, N. Zorn, E. Leize-Wagner, V. Heitz, *Chem. Commun.* **2018**, *54*, 10966–10969.

[14] H.-P. Jacquot de Rouville, C. Gourlaouen, V. Heitz, *Dalton Trans.* **2019**, *48*, 8725–8730.

[15] a) S. Ghosh, A. Wu, J. C. Fettinger, P. Y. Zavalij, L. Isaacs, *J. Org. Chem.* **2008**, *73*, 5915–5925; b) D. Bialas, A. Zitzler-Kunkel, E. Kirchner, D. Schmidt, F. Würthner, *Nat. Commun.* **2016**, *7*, 12949; c) H. Lee, D. Lee, *Commun. Chem.* **2022**, *5*, 180.

[16] a) T. Haino, T. Fujii, Y. Fukazawa, *Tetrahedron Lett.* **2005**, *46*, 257–260; b) T. Haino, T. Fujii, A. Watanabe, U. Takayanagi, *Proc. Natl. Acad. Sci. U. S.A* **2009**, *106*, 10477–10481; c) S. Ibáñez, C. Vicent, E. Peris, *Angew. Chem. Int. Ed.* **2022**, *61*, e202112513; d) M. Yuan, X. Zhang, Y. Han, F. Wang, F. Wang, *Inorg. Chem.* **2020**, *59*, 14134–14140.

[17] a) F. Diederich, *Angew. Chem. Int. Ed. Engl.* **1988**, *27*, 362–386; b) S. B. Ferguson, E. M. Seward, F. Diederich, E. M. Sanford, A. Chou, P. Inocencio-Szweda, C. B. Knobler, *J. Org. Chem.* **1988**, *53*, 5593–5595; c) K. T. Chapman, W. C. Still, *J. Am. Chem. Soc.* **1989**, *111*, 3075–3077; d) D. B. Smithrud, F. Diederich, *J. Am. Chem. Soc.* **1990**, *112*, 339–343; e) D. B. Smithrud, T. B. Wyman, F. Diederich, *J. Am. Chem. Soc.* **1991**, *113*, 5420–5426; f) M. S. Cubberley, B. L. Iverson, *J. Am. Chem. Soc.* **2001**, *123*, 7560–7563.

[18] C. Reichardt, *Chem. Rev.* **1994**, *94*, 2319–2358.

[19] Formation of the N-methylated tweezers (**3·2CF$_3$COO**) and the N-protonated tweezer (**4·2CF$_3$COO**) were performed according to a previously reported strategy (see ESI, Scheme S2.1).

[20] All compounds were characterized by X-ray diffraction (see ESI, section 9).

[21] Crystal data for **2·2Cl**: $C_{43}H_{29}N_3$,2(Cl), yellow prism, crystal size 0.120 × 0.100 × 0.60 mm, tetragonal, space group P 4_2/n, a = 16.3965(3) Å, b = 16.3965(3) Å, c = 13.8463(5) Å, α = 90°, β = 90°, γ = 90°, V = 3722.51(19) Å^3, Z = 4, Z' = 0.5, ρ_{calc} = 1.175, T = 120(2) K, $R_1(F^2 > 2\sigma F^2)$ = 0.0651, wR_2 = 0.2064. Out of 90033 reflection a total of 3322 were unique. Crystallographic data (excluding structure factors) for the structures reported in this communication have been deposited with the Cambridge Crystallographic Data Center as supplementary publication no. CCDC–2290249. Crystal data for **3·2(PF$_6$)**: 2($C_{47}H_{37}N_3O_2$),4(F_6P),5(C_2H_3N), yellow block, crystal size 0.160 × 0.120 × 0.10 mm, triclinic, space group P -1, a = 12.4337(4) Å, b = 15.1604(6) Å, c = 26.6053(10) Å, α = 81.2490(10)°, β = 86.4670(10)°, γ = 76.9900(10)°, V = 4827.53 Å^3, Z = 2, Z' = 1, ρ_{calc} = 1.470, T = 120(2) K, $R_1(F^2 > 2\sigma F^2)$ = 0.0589, wR_2 = 0.1501. Out of 221080 reflection a total of 23118 were unique. Crystallographic data (excluding structure factors) for the structures reported in this communication have been deposited with the Cambridge Crystallographic Data Center as supplementary publication no. CCDC–2290247.

[22] A. B. Grommet, J. B. Hoffman, E. G. Percástegui, J. Mosquera, D. J. Howe, J. L. Bolliger, J. R. Nitschke, *J. Am. Chem. Soc.* **2018**, *140*, 14770–14776.

[23] Phase transfer experiments were ineffective using other solvents ($CDCl_3$, CD_3NO_2) than CD_2Cl_2 or using different acids (DCl, DNO_3) than D_2SO_4.

[24] The completion of the titration was not achieved since precipitation and difficult phase separation decreased shim quality. In addition, the increase of the ionic strength led to a decrease of the overall sensitivity of the NMR experiment.

[25] A similar behavior is observed for all tweezers.

[26] In the lower case, only 3% of ($\mathbf{4^{2+}}$)$_2$ is fully solvated in the H_2O phase.

[27] A. Chaumont, G. Wipff, *J. Comp. Chem.* **2002**, *23*, 1532–1543.

[28] a) J. Hu, J. S. Ward, A. Chaumont, K. Rissanen, J.-M. Vincent, V. Heitz, H.-P. Jacquot de Rouville, *Angew. Chem. Int. Ed.* **2020**, *59*, 23206–23212; b) J. Hu, S. Adrouche, E. S. Gauthier, N. Le Breton, M. Cecchini, C. Gourlaouen, S. Choua, V. Heitz, H.-P. Jacquot de Rouville, *Chem. Eur. J.* **2022**, *28*, e202202840.

[29] a) S. Paliwal, S. Geib, C. S. Wilcox, *J. Am. Chem. Soc.* **1994**, *116*, 4497–4498; b) C. A. Hunter, *Angew. Chem. Int. Ed.* **2004**, *43*, 5310–5324; c) A. M. L. West, N. Dominelli-Whiteley, I. V. Smolyar, G. S. Nichol, S. L. Cockroft, *Angew. Chem. Int. Ed.* **2023**, *62*, e202309682.

[30] A. Gosset, Z. Xu, F. Maurel, L.-M. Chamoreau, S. Nowak, G. Vives, C. Perruchot, V. Heitz, H.-P. Jacquot de Rouville, *New J. Chem.* **2018**, *42*, 4728–4734.

[31] G. R. Fulmer, A. J. M. Miller, N. H. Sherden, H. E. Gottlieb, A. Nudelman, B. M. Stoltz, J. E. Bercaw, K. I. Goldberg, *Organometallics* **2010**, *29*, 2176–2179.

[32] M. Krejčik, M. Daněk, F. Hartl, *J. Electroanal. Chem. Interfacial Electrochem.* **1991**, *317*, 179–187.

[33] "M86-E01078 APEX2 User Manual", Bruker AXS Inc., Madison, USA, **2006**.

[34] G. M. Sheldrick, *Acta Crystallogr.* **2015**, *A71*, 3–8.

[35] G. M. Sheldrick, *Acta Crystallogr.* **2008**, *A64*, 112–122.

[36] D. A. Case, I. Y. Ben-Shalom, S. R. Brozell, D. S. Cerutti, T. E. Cheatham, III, V. W. D. Cruzeiro, T. A. Darden, R. E. Duke, D. Ghoreishi, M. K. Gilson, H. Gohlke, A. W. Goetz, D. Greene, R. Harris, N. Homeyer, Y. Huang, S. Izadi, A. Kovalenko, T. Kurtzman, T. S. Lee, S. LeGrand, P. Li, C. Lin, J. Liu, T. Luchko, R. Luo, D. J. Mermelstein, K. M. Merz, Y. Miao, G. Monard, C. Nguyen, H. Nguyen, I. Omelyan, A. Onufriev, F. Pan, R. Qi, D. R. Roe, A. Roitberg, C. Sagui, S. Schott-Verdugo, J. Shen, C. L. Simmerling, J. Smith, R. Salomon-Ferrer, J. Swails, R. C. Walker, J. Wang, H. Wei, R. M. Wolf, X. Wu, L. Xiao, D. M. York, P. A. Kollman, (**2022**), AMBER 2022, University of California, San Francisco.

[37] J. Wang, R. M. Wolf, J. W. Caldwell, P. A. Kollamn, D. A. Case, *J. Comput. Chem.* **2004**, *25*, 1157–1174.

[38] W. D. Cornell, P. Cieplak, C. I. Bayly, P. A. Kollman, *J. Am. Chem. Soc.* **1993**, *115*, 9620–9631.

[39] M. Baaden, F. Berny, G. Wipff, *J. Mol. Liquids* **2001**, *90*, 1–9.

[40] T. Fox, P. A. Kollman, *J. Phys. Chem. B* **1998**, *102*, 8070–8079.

[41] W. L. Jorgensen, J. Chandrasekhar, J. Madura, R. W. Impey, M. L. Klein, *J. Chem. Phys.* **1983**, *79*, 926–935.

[42] H. J. C. Berendsen, J. P. M. Postma, W. F. van Gunsteren, A. DiNola, J. R. Haak, *J. Chem. Phys.* **1984**, *81*, 3684–3690.

[43] M. P. Allen, D. J. Tildesley, *Computer Simulation of Liquids*, Oxford Science Publications, **1987**.

Manuscript received: May 13, 2024
Accepted manuscript online: May 23, 2024
Version of record online: July 15, 2024